



HAL
open science

pXRF on printed circuit boards: Methodology, applications, and challenges

Solène Touzé, Valérie Laperche, Agathe Hubau, Pauline Moreau

► To cite this version:

Solène Touzé, Valérie Laperche, Agathe Hubau, Pauline Moreau. pXRF on printed circuit boards: Methodology, applications, and challenges. *Waste Management*, 2022, 146, pp.66-76. 10.1016/j.wasman.2022.05.001 . hal-03711366

HAL Id: hal-03711366

<https://brgm.hal.science/hal-03711366v1>

Submitted on 22 Jul 2024

HAL is a multi-disciplinary open access archive for the deposit and dissemination of scientific research documents, whether they are published or not. The documents may come from teaching and research institutions in France or abroad, or from public or private research centers.

L'archive ouverte pluridisciplinaire **HAL**, est destinée au dépôt et à la diffusion de documents scientifiques de niveau recherche, publiés ou non, émanant des établissements d'enseignement et de recherche français ou étrangers, des laboratoires publics ou privés.



Distributed under a Creative Commons Attribution - NonCommercial 4.0 International License

1 **Title:** pXRF on Printed Circuit Boards: Methodology, applications, and challenges

2

3 **Key words:** waste printed circuit board, sampling, characterisation, metals, analysis, urban
4 mining, pXRF

5

6 **Authors:** Solène Touzé¹, Valérie Laperche¹, Agathe Hubau¹, Pauline Moreau¹

7 ¹-BRGM, 3 av. Claude Guillemin, 45060 Orléans, France

8

9 **Abstract :**

10

11 In order to develop methods to determine the chemical composition of Waste Printed
12 Circuit Boards (WPCB), this study focused on the analysis of 10 metals (Cu, Fe, Sn, Zn, Pb, Ni,
13 Sb, Cr, Mo and Pd) using portable X-ray fluorescence (pXRF) compared to ICP-MS
14 measurements after aqua regia digestion . Different experimental conditions were tested: 3
15 particle sizes (200 µm, 750 µm and 2 mm) and 3 sample preparations (tube, cup and loose
16 powder). For each condition tested, 8 to 16 independent replicates were done. ICP
17 measurements with the 200 µm sample, considered as the reference condition in this study,
18 confirmed the homogeneity of the sample at this particle size and the robustness of the
19 sampling protocol (RSD < 5 % for all elements). For this particle size, pXRF has low data
20 dispersion too (Cu, Fe, Sn, Zn, Pb, Sb and Cr showed RSD < 10 %) and the use of loose
21 powder seems to be a sufficient preparatory step. Moreover, the deviation of pXRF

22 measurements with the 200 μm sample from the reference condition was acceptable (<
23 20%) for Cu, Sn, Zn, Pb, Ni, Sb and Mo. For coarser samples, i.e. 750 μm and 2 mm, the
24 homogeneity was much more doubtful, which needs to be offset by a larger number of
25 repetitions. For these particles sizes, pXRF set to factory-installed mining mode did not
26 produce accurate measurements but could provide a rapid non-intrusive approach for first-
27 level screening to assess the relative difference of metal contents between WPCB samples.

28

29

30 **1 Introduction**

31 **1.1. The complexity of Waste Printed Circuit Boards**

32 Our societies generate ever larger masses of electronic waste: more than 53.6 million tonnes
33 of electronic and electrical waste (excluding photovoltaic panels) were produced globally in
34 2019 of which only a small proportion (17.4 %) is formally recycled (Forti et al., 2020).

35 Metals represent a significant part of this waste, both in volume and in material value
36 (UNEP, 2013). The recycling market for old electronic devices is essentially based on
37 recovered metals, recycling chains for plastics, glass and ceramics being more limited.
38 Printed circuit boards are among the most economically relevant waste materials in this
39 category. Various processing units recycle Waste Printed Circuit Boards (WPCB) to capture
40 metals of value, such as Cu, Ag, Au (Ghosh et al., 2015; Rocchetti et al., 2018), but only part
41 of their value is currently being captured (Thomas, 2016; Qui et al., 2021). Incomplete
42 knowledge on the available feedstock is also problematic for establishing alternative metal
43 recovery operations. To obtain reliable values for WPCB metal content, the characterization
44 of materials has to be fully controlled, reproducible and reliable. At present, there is no
45 approved and standardized methodology for WPCB characterization.

46 WPCB is a complex mix of substances, and determining the composition of a pile of WPCB
47 with accuracy requires high quality sampling and analysis. Numerous factors have a strong
48 impact on the values measured and their deviations: sampling (dynamic flow or static pile),
49 physical preparation of the raw material (shredding and dividing steps), sample preparation
50 before analysis (digestion, fusion and pellet preparation), analytical measurement, etc.
51 (Kaya, 2019).

52 The first factors (physical preparation and division) are part of the sampling plan. The e-cards
53 in stacks of WPCB can be several tens of centimetres in size, which is too large to be
54 characterized without shredding. The sampling plan starts with several particle size
55 reduction and splitting steps. The aim of the sampling plan is to supply a sample with a
56 specific mass and specific particle size. Any sampling error has to be associated with each
57 datum on metal content. No sampling plan for WPCB is publicly available: some companies
58 have developed internal procedures, but these are rarely accessible. A plan has been
59 published by the UMICORE smelter, but it is not up-to-date (Hagelüken, 2006; UMICORE,
60 2012). In most scientific papers characterizing WPCB, the material is shredded into particles
61 of one to a few millimetres and in some cases sieved to isolate fine particles (Ogunniyi et al.,
62 2009; Korf et al., 2019), but none provides a sampling plan.

63 The last factors (analytical protocols) are part of analysis methodology. Analyses can be
64 destructive, e.g. fire assay, calcination, digestion required before Inductively Coupled Plasma
65 spectrometry (ICP) or Atomic Absorption Spectrometry (AAS), or non-destructive (loose
66 pellets for XRF or LIBS). Metals in WPCB are often measured with ICP after aqua regia
67 leaching (Kaya, 2019; Korf et al., 2019; Hubau et al., 2019; Ogunniyi et al., 2009; Wienold et
68 al., 2011). This method allows, in a single analysis, the determination of thirty chemical
69 elements and therefore provide substantial information on the composition of the sample.
70 Generally, the digestion step with aqua regia is effective for most metals and allows true
71 values to be approached (Hubau et al., 2019; Ogunniyi et al., 2009; Wienold et al., 2011;
72 Andrade et al., 2019). Digestion has significant drawbacks, however, as it is extremely time-
73 consuming and costly.

74 Hubau et al., (2019) and Touzé et al., (2020) worked on the effects of sample preparation
75 (grain-size, sample masses for digestion, digestion methods, analysis techniques) and the
76 number of repetitions on the quality of results. The results of these studies have shown that
77 the more finely ground the sample, the lower the dispersion of the results (less than 5%).
78 The techniques used for grinding to 200 µm are complex and difficult to adapt for routine
79 sample preparation.

80 **1.2. The portable XRF method**

81 Rapid technological progress in the field of portable X ray fluorescence (pXRF) spectrometry
82 has increased its applications for environmental sample analysis. These instruments can
83 provide cost-effective, non-destructive, real-time, direct on site-measurements of a wide
84 range of inorganic elements in solid samples. X-ray fluorescence spectrometry is a chemical
85 analysis technique using a physical property of matter. When matter is bombarded with X-
86 rays, it re-emits energy in the form, among other things, of X-rays. The spectrum of X-rays
87 emitted by matter is characteristic of the composition of the sample, by analysing this
88 spectrum, we can deduce the elementary composition, that is, the mass concentrations of
89 elements.

90 The pXRF technique is being successfully used in many different disciplines, including
91 environmental remediation (Kalnicky et al., 2001; Laperche et al., 2008; Higuera et al.,
92 2012), recycling, archaeological applications (Cesareo et al., 2009), health and
93 geology/mining (Houlahan et al., 2003). pXRF instruments are designed to analyse very small
94 sample volumes and this can be a source of large analytical errors besides the other factors
95 that influence the quality of pXRF measurements: heterogeneity of the sample, number of
96 shots, surface irregularity and by extension variable path length (Potts, 2008). The latter two

97 derive from the fact that the air gap between the sample and the measurement window
98 dampens the X-ray signal produced by the sample. This often leads to a lower measured
99 concentration (Markowicz, 2008) and if the path length is variable, the lower concentration
100 cannot be countered by a conversion factor.

101 There are two ways to evaluate the measurement results from pXRF: i) sample pXRF
102 measured values versus chemical measured values (Radu et al., 2009) and ii) sample pXRF
103 measured values versus reference material measured values (Peinado et al., 2010). Since
104 06/2019, a certified reference material, BAM-M505a, has been available for the
105 development, validation and quality control of analytical methods and procedures to
106 determine main and trace components in electronic waste (Recknagel, 2019). The way the
107 reference sample is prepared (melted and mixed pyrite) is very different to the way our
108 samples are prepared (no modification of the sample except grinding).

109 Sample preparation is a key parameter to obtain qualitative measurements. Some authors
110 (Goff et al., 2019; Civici, 2005; Zhou et al., 2020) have studied the effect of preparation on
111 soil, sediment and mineral samples for pXRF measurements. pXRF providers recommend
112 gently pressing powder to form pellets (dried – ground – pressed sample), which often
113 produces a better correlation with chemical analysis than samples in loose powdered form.
114 However, there is no consensus on this tendency; in the studies of Goff (Goff et al., 2019),
115 pressed pellets were not the optimum type of sample preparation for some elements (Al and
116 Fe). The inconsistency between sources in the literature underlines the importance of the
117 preparation step because it results in substantial differences between particular matrices
118 depending on the composition and particle size distributions.

119 1.3 Applicability of pXRF to electronic waste

120 As with any new method, researchers are actively seeking to extend its main fields of
121 application. Very little documentation exists on the applicability of pXRF to solid waste; some
122 authors have worked on solid wood waste (Hasan et al., 2011), compost (McWhirt et al.,
123 2012; Havukainen et al., 2019; López-Núñez et al., 2020) and the fine fraction released from
124 solid recovered fuel production (Havukainen et al., 2019). For electronic waste, three
125 authors have used pXRF to characterize printed circuit board samples (Otsuki et al., 2019 and
126 2020; Korf et al., 2019; Recknagel, 2019) and one has worked on electronic WPCB
127 components (Martin et al., 2010).

128 Recknagel has proposed a reference material from ashed WPCBs that were melted with
129 pyrite (Recknagel, 2019). This author used pXRF to test the homogeneity of 30 sub-samples.
130 The analysis results are therefore studied only in relative rather than absolute terms. Due to
131 the matrix preparation (melted and mixed), the material is different to those of interest in
132 this study (Recknagel, 2019). Korf also used pXRF to test the homogeneity of 7 samples
133 (particle sizes < 200µm) of WPCB, and compared pXRF results to ICP results after acid
134 digestion (Korf et al., 2019). The comparison with digestion-ICP showed that for base metals
135 (Cu, Fe, and Zn), pXRF produced comparable results while Sn was overestimated and the
136 platinum group and precious, speciality and hazardous metals were not well analysed.
137 Otsuki used a Niton XL3t GOLDD and cup-prepared sample. He repeated the analysis 5 times
138 for processed samples (size fractions separated by sieving steps) and 20 times for
139 unshredded samples (Otsuki et al., 2019). XRF was compared to Prompt Gamma Activation
140 Analysis (PGAA). Values measured by PGAA for Cu, Fe, Zn and Pb were systematically higher
141 than the values measured by pXRF. Martin evaluated different sampling preparations for the
142 determination of hazardous metals (Cr, Cd, Pb) in WPCB using X-ray fluorescence (EDXRF)
143 (Martin et al., 2010). He compared the XRF measurement of individual electronic

144 components in WPCB before and after grinding. No information was given on the particle
145 size obtained, but it was clearly shown that the metal content measurement increases
146 considerably after a grinding step.

147 Since there are very few studies evaluating the use of pXRF for metal determination in
148 electronic waste, the main objective of this paper is to study the applicability of pXRF to
149 investigate the metal content of heterogeneous WPCB. This was done through a comparison
150 with aqua regia digestion followed by ICP, as reported to be widely used in analytical
151 laboratories. The secondary objectives are to study the effect of the particle size and the
152 sample conditioning on the resulting compositional data. To achieve this, nine WPCB
153 samples were prepared for analysis with 3 different grinding preparations (sample maximum
154 particle sizes 2 mm, 750 μm and 200 μm) and 3 conditioning options (loose powder,
155 compacted in a cup and pressed in a tube). These sizes were chosen because they
156 correspond to various degrees of liberation of the metal parts, according to the literature
157 (Otsuki et al., 2020; Bacher et al., 2017, Guo et al., 2011). It is known that a grinding
158 preparation to 2 mm is not well adapted to pXRF. However, due to the complexity of WPCB
159 grinding, a 2 mm particle size sample was chosen to limit the time- and energy-consumption
160 of the preparation, as it could be performed in industries.

161 Particles size and sample conditioning (singly or in combination) affect the confidence level
162 and therefore the precision of the metal contents obtained for WPCB. The elements of
163 interest selected for this study were the critical and base metals Cu, Fe, Sn, Zn, Pb, Ni, Sb, Cr,
164 Mo and Pd.

165 **2 Materials and methods**

166 **2.1 Sample and sample treatment**

167 The WPCB used for this study were from the Small Waste Electrical and Electronic
168 Equipment (sWEEE) category (audio and video appliances, toys, personal care products,
169 culinary equipment etc.). Approximately 500 kg of waste was collected in an industrial
170 sorting chain by the waste recovery company “Envie 2E Midi-Pyrénées” (France). The wastes
171 were dismantled manually to extract the PCB. The entire sample (485 kg) was first shredded
172 with an industrial cutting mill (Bohmier Maschinen GmbH) to a particle size of less than 30
173 mm. After division, a quarter of the sample (122 kg) was then shredded to a particle size of
174 less than 10 mm. The < 10 mm sample was divided to obtain sub-sample masses of 4 kg;
175 three sub-samples of 4 kg were used for the tests:

- 176 i) Sample shredded to 2 mm : the 4 kg sample was shredded to 2 mm in a lab knife mill
177 (Retsch SM2000);
- 178 ii) Sample shredded to 750 µm : the 4 kg sample was shredded successively to 2 mm, 1
179 mm and 750 µm in the same lab knife mill;
- 180 iii) Sample shredded to 200 µm : the 4 kg sample was shredded to 750 µm in the lab
181 knife mill and sent to the Poittemille Company (Bethune, France) to be milled with a
182 universal grinder (FL1 Poittemille) using 200 µm ring holes.

183 The particle sizes of the different shredding steps were chosen from the UMICORE sampling
184 plan (Hagelüken, 2006) and it was adapted to the devices available at BRGM (Hubau et al.,
185 2019). The losses of material were less than 1% in the procedure to obtain the 2 mm and
186 750 µm samples. The losses associated with the size reduction from 750 µm to 200 µm are
187 unknown. No particles were removed during the shredding steps. The sampling

188 methodology and particle size distribution are detailed in Hubau et al., (2019) and Touzé et
189 al., (2020).

190 2.2 Chemical analysis

191 A split shredded sample of 5 g was digested with aqua regia (HNO₃:HCl 1:3) with a solid to
192 liquid ratio of 1:10. The contact time was about 2h at 200°C. The leaching fraction was
193 filtered through 0.45 µm and analysed by ICP-OES (Horiba Jobin Yvon Ultima 2) and ICP MS
194 (Thermo Scientific X Series). Details on the digestion procedure are given in Hubau et al.,
195 (2019). Digestions were performed on the three particle size samples (200 µm, 750 µm and 2
196 mm). 8 or 16 replicated were done for each particle size. Each digestion was analysed with
197 ICP once. The mean metal content values were calculated for each particle size. Pd was
198 analysed only for the 750 µm sample. ICP measurements on the three particle size samples
199 are denoted as [ICP 2 mm], [ICP 750 µm] and [ICP 200 µm]. For sample [ICP 750 µm], the
200 leaching residues obtained after aqua regia digestion were ground again and digested with a
201 mixture of HF, HCl and HNO₃. The second leaching solution was analysed by ICP.

202 2.3 Portable XRF apparatus

203 All pXRF analyses were performed using the Niton XL3t-980 GOLDD model. This energy
204 dispersive pXRF is fitted with a 50 kV X-ray tube (max. 50 kV, 100 µA, 2 W) with an Ag anode
205 target excitation source and a Large Drift Detector (LDD). The spot analysed had a diameter
206 of 8 mm. As part of the standard set-up routine, the analyser was initially energy-calibrated
207 using the embedded silver target to avoid contamination. The source count time for the
208 analysis was set at 30 seconds for the main filter and 120 s for the total analysis using the 4
209 factory-installed filters of the pXRF in the laboratory. All analyses were carried out using the

210 mining mode calibration set by the manufacturer. The resolution of this pXRF is between
211 0.150 and 0.157 keV.

212 2.4 Sample preparation for pXRF

213 The compactness and particle size of the sample are key points in sample preparation as
214 they can affect the metal content measurement. This is even more true for waste with a
215 highly heterogeneous distribution of materials.

216 The samples were prepared using three different preparation procedures (Figure 1):

217 (a) "Tube": The sub-samples from < 0.2 and < 0.75 mm samples were put into a
218 plastic tube for analysis ($\varnothing = 18$ mm; $h = 30$ mm; sample mass $m \approx 10$ g). Sub-
219 sampling was done by grab sampling then compacted in a tube with a press. The
220 tube is positioned upside down on the lab bench during measurements.

221 (b) "Cup": The sub-samples from each sample were put into a plastic cup covered by
222 a thin Prolene™ film ($4 \mu\text{m}$) for analysis ($\varnothing = 26$ mm; $h = 20$ mm; $m \approx 10$ g). Sub-
223 sampling was done by grab sampling. The cup is positioned upside down on the
224 lab-bench during measurements.

225 (c) "Loose powder": The sample was loosened into a heap that was flattened to fill
226 up the tray. A 16-hole plate was positioned on top of the loose powder sample.
227 The measurements were made with the pXRF directly over each hole of the plate.

228 In cases (a and b), 16 cups and 16 tubes were filled for each sample with only one replicate
229 for each cup and tube. In case (c), 16 measurements were made over the whole surface of
230 the loose powder sample with only one replicate for each spot. The manufacture of the 16-
231 hole plate (Figure 1-c) made it possible to respect the geometry: when working on powdery

232 materials without protecting the nose of the device with the metal plate equipped with a
233 Kapton's window, material will enter the circular hole of the analyser.

234 The design of the pXRF is such that the axis of the detector and the axis of the tube meet at
235 the same point. This point corresponds to the analytical distance at which the sample must
236 be placed for the elements to be properly quantified (this is especially true for low-energy
237 elements ranging from Mg to Ca). If there is powder in the circular hole, the analytical
238 distance at which the sample is placed is shorter than it should be, and the values will
239 probably be overstated.

240 The pXRF measurements on the 3 particle size samples and 3 conditioning preparations are
241 denoted as [pXRF Size fraction Conditioning]. For sample [pXRF 2 mm Cup] is a sample
242 analysed by pXRF on 2 mm samples with a cup conditioning.

243 2.5 Experimental protocol and data analysis

244 In order to understand the effects of particle size and material conditioning on the accuracy
245 of metal content determination, 3 different particle size samples (200 μm , 750 μm and 2
246 mm) and 3 different pXRF conditioning options (loose powder, cup and tube) were studied.
247 Combining these two parameters produced nine different conditions. One of the conditions
248 [pXRF 2 mm tube] was abandoned as it was not possible to fill up a tube with 2 mm sample
249 material and have a proper sampling surface. To be able to perform statistical tests, it was
250 decided to repeat each condition at least 16 times, with each metal content value
251 representing one measurement.

252 The first stage in data processing produced simple summaries about the sample and the
253 measurements (arithmetic mean, median and Relative Standard Deviation (RSD) values).
254 These results are presented in Table 2, Table 3, Figure 2 and Figure 4. To identify a potential

255 nugget effect and its impact on the data, it was decided to keep intact data sets (no erratic
256 points were excluded) for this first observation step.

257 The second data processing stage involved statistical tests and calculating the deviation from
258 a reference. To perform these calculations, individual values falling outside the overall
259 pattern of the data set were excluded, which enabled us to obtain normality for the dataset.

260 An erratic point is an observation which is outside the general scope of the other
261 observations. Interquartile Range method (IQR method) was used to identify these points,
262 any values that fall outside of “calculated range” are considered outliers. For one set of data
263 of one condition (1 size particle, 1 conditioning), the two limits are calculated by the
264 equation ($Q1 - 1.5 \cdot IQR$, $Q3 + 1.5 \cdot IQR$), where $Q1$ is the 25th percentile, $Q3$ is the 75th
265 percentile and IQR is the Inter Quartile Range ($IQR = Q3 - Q1$). The 25th percentile is the value
266 at which 25% of the answers lie below that value and 75% of the answers lie above that
267 value, 75th percentile is the value at which 25% of the answers lie above that value and 75%
268 of the answers lie below that value. Mann-Whitney statistical tests were performed to
269 compare the equality of means in two independent samples. This test was chosen because
270 the variances of the results are unequal and the number of samples are less than 30. The
271 tests were performed using XLSTAT with a 95% confidence interval.

272 In the present study, [ICP 200 μm] was employed for the cross-validation to assess the
273 reliability of pXRF for all metals except for Pd, which is compared to [ICP 750 μm]. At the
274 end, 2 sets of ICP results ([ICP 750 μm] and [ICP-2 mm]) and 8 sets of XRF results were
275 compared to [ICP 200 μm] sample data; ICP values are considered as the reference values in
276 this study. The deviation of metal content from the reference technique is calculated using
277 the following equation (1):

278

$$279 \quad \textit{Deviation from reference} = 100 * \frac{[Metal]_{ref} - [Metal]_i}{[Metal]_{ref}}$$

280 (1)

281 Where :

282 $[metal]_{ref}$ = metal content of sample [ICP 200 μ m]

283 $[metal]_i$ = metal content of condition i (1 particle size, 1 conditioning)

284

285 When plotted, this clearly shows the pattern of the individual differences and allows the
286 limits of each technique to be calculated.

287 **3 Results**

288 **3.1 Pre-selection of metals**

289 Analysis by pXRF has certain limitations due to internal Limits of Detection (LOD) (Thermo
290 Scientific, 2010) and potential interferences. The first step in this study was to shortlist
291 metals for comparison. The metal selection was based on: i) known pXRF interferences, ii)
292 comparisons of metal content with the mean values from the ICP analysis ([ICP 200 μ m], [ICP
293 750 μ m] and [ICP 2 mm]) and iii) pXRF LOD (Table 1). LODs are calculated as three standard
294 deviations (99.7% confidence interval) for each element, using 60-second analysis time per
295 filter on well prepared samples (particle size < 74 μ m). The AS acronym means Application
296 Specific; pXRF could be developed but not operationally in our case. The following elements
297 are common to the ICP and XRF analyses: Ag, Al, As, Au, Cd, Co, Cr, Cu, Fe, Mg, Mn, Mo, Nb,
298 Ni, Pb, Pd, Sb, Se, Sn, Sr, V, W, Zn.

299 Aluminium was selected to exemplify the overlap problem. For Al analysis, there was a Br
300 line overlap. Brominated compounds have been used extensively for several decades in the
301 manufacture of printed circuit boards. A brominated flame retardant is primarily used to
302 meet fire safety standards for PCB assemblies. The Br content range is quite large in
303 materials of this type, from 0 to 11 % by weight (Sharkey et al., 2018). The pXRF used in this
304 study was not able to quantify Br but the $K\alpha$ and $K\beta$ X-rays lines for these elements were
305 intense and easily identified on all spectra. Whatever the Br content in our samples, light
306 elements such as Al are only quantified from the K lines ($K\alpha = 1,487$ keV and $K\beta = 1,557$ keV),
307 which have low energy and generate a weak signal but are also close to the L lines of the
308 heavier elements such as Br ($L\alpha=1.480$ keV and $L\beta = 1.526$ keV). The energy resolution of
309 pXRF devices is approximately 0.15 keV and does not allow the K and L lines to be
310 distinguished from each other. Therefore, Al cannot be properly quantified by pXRF in this
311 type of sample.

312 Whether this is due to overlapping lines or to very large differences in contents between
313 different elements, it was not possible to properly quantify Ag, As, Au, Cd and Co in this
314 sample in addition to Al.

315 Only the pXRF results for Cr, Cu, Fe, Mo, Ni, Pb, Pd, Sb, Sn and Zn will be discussed in the
316 following section. A part of the metals selected are found in high concentrations in PCBs with
317 concentrations around several weight percentages (Cu, Sn, Fe, Pb, Ni and Zn), the rest of the
318 metals (Cr, Co, Mo, and Pd) are sparsely distributed with part per million (ppm) content
319 (Bizzo et al. 2014).

320 3.2 Chemical analysis by ICP

321 Three samples with distinct particle size distributions (200 μm , 750 μm and 2 mm) were
322 analysed by ICP. One way of highlighting the influence of these different particle sizes is to
323 compare the mean values of the different conditions (Table 2). In the table, the deviation is
324 expressed in terms of the Relative Standard Deviation (RSD).

325 The mean concentrations obtained for [ICP 750 μm] and [ICP 2 mm] were compared to those
326 obtained for the [ICP 200 μm]. Consistency was very high (deviation <10%) for Fe, Zn, Pb and
327 Ni. For Cr and Mo, there was a tendency towards underestimation when the particle size
328 increased, with deviations of up to 76% for Mo at 2 mm. The tendency was less clear for Cu,
329 Sn and Sb, with variations ranging from 11 to 32%. For Cu and Sn in particular, the
330 concentrations measured for [ICP 750 μm] were lower than those measured for 2 mm.

331 3.2.1 Digestion efficiency

332 For a same digestion condition (5g-2h), the samples with coarse fractions (2 mm and 750
333 μm) could be digested by aqua regia more slowly than the sample with fine fraction (200
334 μm) because of the smaller corresponding surface accessible to leaching reagents. In order
335 to verify the efficiency of the digestion process, the leaching residues (obtained after aqua
336 regia digestion) of the 750 μm sample were ground again, digested with an acid mixture
337 containing HF and analysed. The analytical procedure for this second digestion and the
338 results are described in Hubau et al., (2019). The analysis revealed a percentage of metal
339 recovered from the first digestion above 94% for Cu, Fe, Sn, Zn, Pb and Ni. According to the
340 second digestion methodology developed by Hubau (Hubau et al., 2019), the percentages of
341 metal recovered from the first digestion for Mo and Cr were 98% and 99% respectively for
342 the 750 μm sample. It may thus be assumed that these metals were fully leached from the
343 750 μm sample. The hypothesis of incomplete digestion due to the difference in particle size

344 is therefore rejected for these metals. Our results are consistent with those of Touzé for Ni,
345 Co, Fe, Co, Pb and Zn (Touzé et al., 2020).

346 However, the digestion measured for Sb was incomplete, with 73% of the metal recovered in
347 the first digestion (Hubau et al., 2019). The mean values are thus under-estimated. The low
348 recovery rate of Sb by aqua regia was also observed by Korf (Korf et al., 2019).

349 The difference in magnitude for Sn, Sb, Cr and Mo probably reflects the sample
350 heterogeneity for these elements.

351 3.2.2 Repeatability

352 For all metals, the RSD are below 4% for the [ICP 200 μm]. Therefore, for 16 independent
353 repetitions, we can assume that the 200 μm samples are homogeneous and the sampling
354 procedure is robust. The RSD for the base metals Cu, Fe and Al remain lower than 10% for
355 the [ICP 750 μm] and [ICP 2 mm]. The content of these metals is high enough to remove the
356 disparities arising from particle size with 16 repetitions. For less concentrated metals
357 (content < 5% mass), the RSD varied from 12% to 37% for the [ICP 750 μm] (except for Mo
358 and Sb) and from 11% to 38% for the 2 mm sample (except for Mo). [ICP 750 μm] and [ICP 2
359 mm] are too coarse to obtain a low data spread for the content of metals with low
360 concentrations; to improve the RSD, the mass digested must be > 5 g. This appears to be
361 even more important for Mo at [ICP 750 μm] and [ICP 2 mm], with an RSD above 100%: the
362 very low content results in a very high deviation. The RSD for most metals decreases with
363 particle size (2 mm > 750 μm > 200 μm). These results are consistent with a previous study
364 for Ni, Fe, Cu, Co, Pb and Zn (Touzé et al., 2020), which used the same samples (200 μm , 750
365 μm and 2 mm) analysed with Flame Atomic Absorption Spectrometry (FAAS). This

366 observation may seem obvious if related to good sampling and analysis practices, but it
367 allows deviations to be quantified.

368 3.2.3 Distribution discontinuity

369 The distribution of values is presented as a scattergram, a visual representation of the data
370 that makes it easy to detect distribution irregularities. The scattergrams for the Ni and Mo
371 analyses are presented in Figure 2, which shows interesting anomalies for these two metals.
372 In the scattergrams, each metal content is represented by a black dot; the lines represent
373 median values and the crosses represent mean values. Figure 2 shows 4 erratic points for
374 Mo, with 465 mg/kg and 474 mg/kg for [ICP 750 μm] and 138 and 300 mg/kg for [ICP 2 mm],
375 while the mean values are respectively 158 mg/kg and 44 mg/kg. These 4 points indicate the
376 presence of nuggets of Mo in the digested sample. They are not anomalous and as described
377 in section 0, it is important to keep them in the original data set. Mo could be present in
378 single flakes that form highly concentrated particles with a very significant impact on the
379 measured Mo content. For [ICP 750 μm], the number of repetitions was limited to 8, so that
380 the presence of 2 erratic points has a considerable impact on the mean value. If these 2
381 nuggets are not taken into account for the mean calculation, the mean value is equal to 54
382 mg/kg instead of 158 mg/kg. For [ICP 2 mm], the large number of repetitions ($n = 16$)
383 reduces the impact of the erratic point. No erratic point was observed in [ICP 200 μm].

384 One erratic point was also detected in [ICP 2 mm] for Ni, with a value of 1.02 % for a mean
385 value of 0,46 %. As in the Mo case, for [ICP 2 mm] sample, the number of repetitions ($n = 16$)
386 was sufficient to observe the impact of erratic points on the mean value. In the Touzé study,
387 nuggets were also identified in Ni distributions (Touzé et al., 2020), which highlights the
388 importance, for a critical examination the data set, of carrying out a large number of

389 repetitions and observing the data deviations. No erratic points were detected with the
390 other metals.

391 3.2.4 [ICP 200 μm] as a reference

392 As described in section 0, it was decided to compare [ICP 750 μm] and [ICP 2 mm] to [ICP
393 200 μm]. Erratic points (nuggets) were removed from the data set for these comparisons.
394 Mann Whitney statistical tests showed no significant differences between the values for [ICP
395 200 μm] and [ICP 750 μm] for Zn and Pb, and [ICP 2 mm] for Fe, Zn, Pb and Ni, but a
396 significant difference for the other conditions. The spread of the measurement values for
397 [ICP 200] μm is relatively low (RSD < 4), which leaves little opportunity for not rejecting the
398 test hypothesis.

399 For [ICP 750 μm] and [ICP 2 mm], the deviation from the reference is less than 10% for Fe, Zn
400 and Pb, between 10% and 20% for Cu and greater than 20% for Cr and Mo (Figure 3). The
401 deviations for Ni, Sn and Sb are dependent on the sample conditions: the Ni deviation
402 remains below 12% for both conditions, the Sn deviation varies from 11% [ICP 2 mm] to 33%
403 [ICP 750 μm] and the Sb deviation varies from 17% [ICP 750 μm] to 32% [ICP 2 mm].

404 Preparation by partial grinding to 750 μm and to 2 mm has little impact on the quality of the
405 measurement for Fe, Zn, Ni and Pb, a moderate impact for Cu and a strong impact for Sn, Sb
406 Mo and Cr.

407 3.3 Analysis by portable XRF

408 3.3.1 Mean value and dispersion according to sample preparation

409 Three different sample preparations (tube, cup and loose powder) and 3 particle sizes (200
410 μm , 750 μm and 2 mm) were studied. Combining these two parameters produced 8

411 conditions for study (no data for tube preparation with 2 mm, as explained in 2.5).
412 Evaluation of the data was based first on a comparison of average and relative standard
413 deviations. Mean value and RSD were calculated from 16 measurements, except for 3 loose
414 powder samples because a part of the values were below the Limite Of Detection (LOD); 4
415 measurements for Pd [pXRF 750 μm Powder], 9 measurements for Pd [pXRF 2 mm Powder]
416 and 11 measurements for Mo [pXRF 2 mm Powder] (Table 3).

417 For the 200 μm sample, the mean value does not vary, regardless of the sample preparation.
418 The particle size is fine enough not to be dependent on compaction of the sample. These
419 results are consistent with Zhou's study (Zhou et al., 2020), which concluded that
420 compactness has a modest impact on Fe measurements of a ground mineral sample (80% of
421 particle size below 74 μm). For the 200 μm sample, the RSD is lower than 9% for the 3
422 conditioning preparations except for Mo and Pd (and Cr for the loose powder preparation
423 only). The high RSD for Mo and Pd (16 and 19% both for the 200 μm sample) are due to
424 sample heterogeneity and low concentration. As indicated earlier, sampling error is affected
425 by the concentration of the element studied; it is acknowledged that the error tends to
426 increase with a decreasing metal content. In this study, the Mo and Pd content was very low
427 (Mo = 89 mg/kg and Pd = 21 mg/kg) compared to the other elements. The RSD obtained for
428 the 200 μm sample with cup preparation are consistent with Korf (Korf and al. 2019), where
429 the RSD ranged from 3 to 8 % for Cu Fe Sn Pb Zn and Sb, while the RSD for Pd was 14%.

430 For the 750 μm and 2 mm samples, the contents of elements in the loose powder samples
431 are almost systematically lower than those prepared in cup and tube. The volume analysed
432 in the loose powder samples contains more air than the other preparations (cup and tube)
433 due to the lower compaction constraint. The sample volume for pXRF analysis is defined, so

434 the larger pore volume in a loose powder sample attenuates the signal and the value
435 obtained is therefore lower. For these two samples, the RSD for loose powder was
436 systematically higher than for cup and tube except with Ni, Cr and Pd. The masses used to
437 analyse the cup and tube preparations were larger than for the loose powder preparation
438 because of the different pore volume ratio. This has an impact on the sampling error: the
439 smaller masses used for analysis increase the sampling error and thus data dispersion (Touzé
440 et al., 2019). Furthermore, pXRF analyses the particles present in front of the analysis
441 window. With coarse samples (> 2mm), large grains may dominate the window area and
442 may not be representative of the overall composition.

443 3.3.2 Mean value and deviation according to particle size

444 For each preparation, the element content decreases significantly as the particle size
445 increases.

446 For Cu, Fe, Ni, Sb and Pd, the difference between mean values is slight (for example for Ni,
447 the mean values are 3727 mg/kg for [pXRF 200 µm Cup], 3610 mg/kg for [pXRF 750 µm Cup]
448 and 3461 mg/kg for [pXRF 2 mm Cup]). For other metals (Sn, Zn and Pb) the difference is
449 quite large; this is the case for Zn (the mean values are 2.20 mg/kg for [pXRF 200 µm Cup],
450 1.22 mg/kg for [pXRF 750 µm Cup] and 0.88 mg/kg for [pXRF 2 mm Cup]). Finally, the
451 differences are critical for Mo and Cr (for Cr the mean values are 885 mg/kg for [pXRF 200
452 µm Cup], 597 mg/kg for [pXRF 750 µm Cup] and 282 mg/kg for [pXRF 2 mm Cup]). These
453 results show that pXRF measurements are not only affected by the preparation but are also
454 related to the metals. The grinding step could be selective as different type of metals and
455 other components are ground differently: for example, some metals (lead and copper) are
456 often beaten into flakes or smeared onto grinding surfaces and not well ground. This causes

457 greater variation in metal particle size, which leads to significant problems with particle
458 dispersion. This may affect the extent of metal release, in fact some metals might be
459 released and accessible to surface analysis whereas others might be trapped and
460 inaccessible. This effect is amplified for coarse particles.

461 In any case, there is an underestimation of metal contents for the coarsest sample. Assuming
462 that the average composition of the sample is the same for the three “particle size” samples,
463 the difference between samples could be explained by the variation of the pore volume
464 ratio. As this ratio increases with particle size, the 2 mm sample has the lowest ratio of the
465 three samples. As indicated in section 3.3.1, the presence of a larger pore volume in a
466 sample attenuates the signal and the value measured is therefore underestimated.
467 Obviously, this also applies to the impact of particle size on data dispersion: the RSD
468 increases when particle size increases.

469 Our results are consistent with part of the Civici study (Civici, 2005). This author compared
470 the influence of particle size on pXRF measurements of polluted ground sediment; 4 particle
471 sizes between 2 mm and 150 μm were tested (the 2 mm sample contained 50 to 70% of fine
472 particles < 150 μm). In this study, the metal content decreased as the particle sizes increased
473 for Cu and Zn (ppm level) but not for Fe (% level).

474 3.3.3 Presence of metal nuggets

475 As with the ICP results, few erratic points (Figure 4) were observed for some elements,
476 including Mo ([pXRF 750 μm Cup] – average: 44 mg/kg, erratic point: 123 mg/kg), Ni ([pXRF
477 750 μm Tube] - average: 0.36 mg/kg, erratic point: 1.6 %), Cr ([pXRF 750 μm Cup], average:
478 597 mg/kg, erratic point: 1954 mg/kg) and Pd ([pXRF 2 mm Cup] – average: 29 mg/kg, erratic
479 point 157 mg/kg). These points are not anomalous and it is important to keep them in the

480 original dataset as they indicate the presence of nuggets in the prepared sample. If these
481 nuggets are not taken into account, the RSD decreases from 53 to 27% for Mo, from 83 to
482 15% for Ni, from 64 to 23% for Cr and from 130 to 38 % for Pd. The number of repetitions
483 (n = 16) is sufficient to observe the impact of erratic points on mean values. Again, this
484 highlights the importance, to evaluate the dataset, of carrying out a large number of
485 repetitions and observing the data deviations.

486 3.3.4 Spectral analysis

487 The pXRF spectra were inspected visually in order to ascertain the significance of any
488 interference arising from energy peak overlaps and to study the effect of sample
489 preparations. No unknown interference was identified but some effects of particle size were
490 detected.

491 Unlike other particle sizes where only variations in intensity are observed, considerable
492 variations in intensity were observed in the case of 2 mm samples (Ca Fe, Cu and Br) as well
493 as the appearance or disappearance of certain lines corresponding to P, Al, Cl, Co, Ni, etc.
494 The intensity of the X-rays emitted varies significantly depending on the particle size
495 distribution. With large grains, X-rays provide information on the specific composition of the
496 elements contained in these grains, while with small particle samples, the information
497 received will be representative of the general composition.

498 Furthermore, when the grains are large, the X-rays emitted are partially reabsorbed, and can
499 be completely absorbed in some cases (opacifying effect). The sensitivity of the
500 spectrometer varies depending on the distance between the X-ray tube and the sample. The
501 flatness of the preparation should therefore be as perfect as possible

502 In summary, the sample conditioning mode (Inotedoose powder, cup, and tube) have no
503 impact on the contents and dispersion when the sample is finely ground (< 200 µm).
504 However, conditioning mode do have an impact on contents and dispersion for coarse
505 particle sizes (750 µm and 2 mm). The contents for loose powder samples are systematically
506 lower than for samples prepared in tubes and cups. Loose powder RSD are higher than for
507 cup and tube samples for most elements. The sample particle size has an impact on the
508 contents for all 3 preparations: for the majority of the elements, the metal contents [pXRF 2
509 mm Cup/Powder] [pXRF 750 µm Tube/Cup/Powder] are lower than [pXRF 200 µm
510 Tube/Cup/Powder]. The RSD systematically increases (besides the nugget effect) from [pXRF
511 2 mm Cup/Powder] > [pXRF 750 µm Tube/Cup/Powder] > [pXRF 200 µm Tube/Cup/Powder].
512 Measurements for [pXRF 750 µm Tube/Cup/Powder] and [pXRF 2 mm Cup/Powder] are
513 systematically underestimated. Samples for analysis should be ground to 200 µm at least.

514 3.4 [ICP 200 µm] reference versus pXRF

515 The study as a whole made more than 100 values available for each metal. Table 3 shows the
516 mean metal contents for each condition measured by pXRF. To compare them, each
517 condition was compared to a reference value represented by [ICP 200 µm] (Table 2), except
518 for Pd where the reference sample was [ICP 750 µm]. In Figure 5, individual values falling
519 outside the overall pattern of the data set were excluded; “n” indicates the number or
520 repetition after point exclusion. For Sb, the values obtained by ICP ([ICP 200 µm]) are
521 underestimate, only 73% of the metal were recovered by aqua regia digestion (section
522 3.2.1). The Sb reference value used in this section was recalculated from this rate (2393 ppm
523 instead of 1742 ppm).

524 Mann Whitney statistical tests showed that only four pXRF conditions produced no
525 significant difference between [ICP 200 μm] values: Pb for [pXRF 200 μm Tube], Mo for
526 [pXRF 200 μm Powder] and [pXRF 200 μm Cup] and Ni for [pXRF 2 mm Cup]. As mentioned
527 previously, the low spread of data for [ICP 200 μm] leaves little opportunity for not rejecting
528 the test hypothesis. For Pd there are no significant differences between [ICP 750 μm] and
529 [pXRF 200 μm Tube/Cup/Powder] values. The spread of Pd for [ICP 750 μm] values is large
530 (RSD = 37%), which does leave more room to accept the test hypothesis.

531 Korf also compared pXRF to ICP (Korf et al., 2019). In this study, only the undersized sieved
532 fractions were selected (< 200 μm): the un-ground fraction was not take into account. Two
533 different laboratories carried out the tests with a NITON XL3t (MINING and PLASTIC modes)
534 and a NITON XL3t-Air (MINING mode) and the materials were prepared in cups. The
535 comparison results are very close to ours: Korf pXRF values showed significant differences
536 from ICP analysis for Cu, Fe, Sn, Zn, Sb, Pb and Pd.

537 For the 10 elements, the [pXRF 750 μm Tube/Cup/Powder] and [pXRF 2 mm Cup/Powder]
538 deviation from the reference [ICP 200 μm] is greater than 20% whatever the conditioning
539 mode (except for Sb and Ni [pXRF 2 mm Cup] where the deviation is 18%), (Figure 5). For
540 [pXRF 200 μm Tube/Cup/Powder] Cu, Sn, Zn, Ni and Pd have a weight difference of less than
541 20% compared to [ICP 200 μm]; Pb, Sb and Mo have a weight difference of less than 10%.
542 For Cr, and Fe, the weight difference is always greater than 20%. For the pXRF and ICP
543 comparison, Korf obtained similar results for Cu, Sn, Zn, Pb and Sb but different results for Fe
544 and Pd (Korf et al., 2019).

545 Therefore, for our sample, it is acceptable to use pXRF set to mining mode to measure Cu,
546 Sn, Zn, Ni, Pd, Pb, Sb and Mo as long as the sample is ground to 200 μm . In this case, the

547 deviations remained within acceptable limits (< 20% weight difference compared to ICP
548 analysis), the Cu, Sn, Pb Ni, and Pd values being slightly underestimated and Zn and Sb
549 slightly overestimated. Whatever the preparation, it seems that the use of pXRF, with
550 factory-installed mining mode calibration, is not recommended for Cr and Fe measurements.
551 Correction of the matrix effect is limited for this type of sample.

552 Additional studies must be conducted to optimize the calibration process with samples with
553 multiple concentration levels and with standards when they become available. The
554 collection of new data could allow post-analysis calibrations for Cr and Fe and for samples
555 ground to 750 µm.

556 **4 Conclusion**

557 This study enabled us to acquire data on the analysis of 10 metals (Cu, Fe, Sn, Zn, Pb, Ni, Sb,
558 Cr, Mo and Pd) contained in WPCB, using pXRF measurements as compared to the
559 frequently used aqua regia digestion followed by ICP. Three particle sizes (200 µm, 750 µm
560 and 2 mm) and three preparations for pXRF (tube, cup and loose powder) were tested.

561 The study has shown that pXRF can be a useful tool for the quantification of Cu, Sn, Zn, Ni,
562 Pd, Pb, Sb and Mo in WPCB with factory-installed mining mode calibration: less than 20%
563 deviation between pXRF and the reference [ICP 200 µm]) was obtained. Practical limits exist
564 on the preparation of samples, which have to be ground to 200 µm to produce acceptable
565 results. On the other hand, for Cr and Fe, pXRF with the factory-installed mining mode
566 calibration does not produce accurate measurements of these metals in WPCB; deviations
567 from the reference [ICP 200 µm] being > 20%. The preparation of the samples (tube, cup or
568 loose powder) is not critical and has little impact on the quantification of Cu, Sn, Zn, Ni, Pd,

569 Pb, Sb and Mo. Therefore pXRF can provide cost-effective, non-destructive, real-time, direct
570 on site-measurements for some metals when WPCB are ground to 200 µm.

571 For coarser samples (750 µm and 2 mm), pXRF does not produce accurate measurements of
572 the metal content of WPCB with factory-installed mining mode calibration: more than 20%
573 deviation from the reference was observed expect for Sb. Particle size strongly influences
574 the homogeneity of the sample (RSD increases with larger particle sizes, as with the ICP
575 methodology) and the intensity of the X-rays emitted (concentrations decrease when
576 particle sizes increase). For these samples, the mode of preparation has an effect on the
577 dispersion of data: RSD are higher for loose powder than for cup and tube preparations.
578 Even so, for coarse samples, pXRF is a rapid and non-intrusive approach that can be used as
579 a first-level screening method to assess the relative distribution of metals in WPCB. Despite
580 these results, pXRF can be relevant with suitable calibration.

581 More investigations on these elements with pXRF would be necessary for different types of
582 WPCB, in order to modify the calibration factors for each element of interest. Suitably
583 calibrated, pXRF would be able to give values comparable to those of laboratory methods.
584 The larger the number of samples, the more robust the calibrations obtained.

585

586 **5 Bibliography**

587

588 Andrade, D.F., Cardoso Machado, R., Arruda Bacchi, M., Pereira-Filho, E.R., 2019. Proposition
589 of electronic waste as a reference material – part 1: sample preparation, characterization
590 and chemometric evaluation. *J. Anal. At. Spectrom.* 34, 2394–2401.
591 <https://doi.org/10.1039/c9ja00283a>.

592 Bachér, J., Kaartinen, T., 2017. Liberation of Printed Circuit Assembly (PCA) and dust
593 generation in relation to mobile phone design in a size reduction process. *Waste Manag.* 60,
594 609-617. <https://doi.org/10.1016/j.wasman.2016.09.037>

595 Bizzo, W.A., Figueiredo, R.A., Andrade, V.F., 2014. Characterization of Printed Circuit Boards
596 for Metal and Energy Recovery after Milling and Mechanical Separation. *Materials.* 7, 4555–
597 4566. <https://doi.org/10.3390/ma7064555>

598 Cesareo, R., Bustamante, A. D., Julio Fabian, S., Calza, C., Anjos, M., Lopes, R. T., Alva, W.,
599 Chero, L., Gutierrez, V. F., Espinoza, M. D., Rodriguez, R. R., Seclen, M. F., Curay V., Elera, C.,
600 Shimada I.. Pre-Columbian alloys from the royal tombs of Sipán and from Museum of Sicán:
601 non-destructive XRF analysis with a portable equipment. *Archéo Sciences* 2009, 33, 281–
602 287. <https://doi.org/10.4000/archeosciences.2323>.

603 Civici, N., 2005. Influence of sample preparation on the analytical performance of fpXRF in
604 connection with geochemical mapping requirements. In IAEA, *In Situ Applications of X Ray
605 Fluorescence Techniques*; IAEA-TECDOC-1456 (ISBN:92-0-107105-1). Available online:
606 [http://www-pub.iaea.org/books/IAEABooks/7212/In-SituApplications-of-X-Ray-
607 Fluorescence-Techniques](http://www-pub.iaea.org/books/IAEABooks/7212/In-SituApplications-of-X-Ray-Fluorescence-Techniques) (accessed on 26 april 2021).

608 Forti, V., Baldé, C.P., Kuehr, R., Bel, G., 2020. The Global E-waste Monitor 2020: Quantities,
609 flows and the circular economy potential. United Nations University (UNU)/United Nations
610 Institute for Training and Research (UNITAR) – co-hosted SCYCLE Programme, International
611 Telecommunication Union (ITU) & International Solid Waste Association (ISWA),
612 Bonn/Geneva/Rotterdam.

613 Ghosh, B., Ghosh, M.K., Parhi, P., Mukherjee, P.S., Mishra, B.K., 2015. Waste printed circuit
614 boards recycling: an extensive assessment of current status. *J. Clean. Prod.* 94, 5–19.
615 <https://doi.org/10.1016/j.jclepro.2015.02.024>.

616 Goff, K., Schaetzl, R.J., Chakraborty, S., Weindorf, D.C., Kasmerchak, and C., Bettis, E.A.,
617 2019. Impact of sample preparation methods for characterizing the geochemistry of soils
618 and sediments by portable X-ray fluorescence. *Soil Science Society of America Journal.* 84,
619 131-143 <https://doi.org/10.1002/saj2.20004>.

620 Guo, C., Wang, H., Liang, W., Fu, J., Yi, X., 2011. Liberation characteristic and physical
621 separation of printed circuit board (PCB). *Waste Management.* 31, 2161-2166.
622 <https://doi.org/10.1016/j.wasman.2011.05.011>

623 Hagelüken, C., 2006. Improving metal returns and eco-efficiency in electronics recycling - a
624 holistic approach for interface optimisation between pre-processing and integrated metals
625 smelting and refining. In: *Proceedings of the 2006 IEEE*, pp. 218–223.

626 Hasan, A.R., Solo-Gabriele, H., Townsend, T., 2011. Online sorting of recovered wood waste
627 by automated XRF-technology: Part II. Sorting efficiencies. *Waste Manage.* 31, 695–704.
628 <https://doi.org/10.1016/j.wasman.2010.10.024>.

629 Havukainen, J., Hiltunen, J., Puro, L., Horttanainen, M., 2019. Applicability of a field portable
630 X-ray fluorescence for analyzing elemental concentration of waste samples. *Waste Manag.*
631 83, 6–13. <https://doi.org/10.1016/j.wasman.2018.10.039>.

632 Higuera, P., Oyarzun, R., Iraizoz, J.M., Lorenz, S., Esbrí, J.M., Martínez-Coronado, A. 2012.
633 Low-cost geochemical surveys for environmental studies in developing countries: testing a
634 field portable XRF instrument under quasi-realistic conditions. *J. Geochem. Explor.* 113 3-12.

635 Houlahan, T., Ramsay, S., Povey, D. 2003. Use of Field Portable X-Ray Fluorescence Spectrum
636 Analyzers for Grade Control – A Presentation of Case Studies. In: 5th International Mine
637 Geology Conference. Australasian Institute of Metallurgy. 377–385.

638 Hubau, A., Chagnes, A., Minier, M., Touzé, S., Chapron, S., Guezennec, A.G., 2019. Recycling-
639 oriented methodology to sample and characterize the metal composition of waste Printed
640 Circuit Boards. *Waste Manage.* 91, 62–71. <https://doi.org/10.1016/j.wasman.2019.04.041>.

641 Kalnicky, D., Singhvi, R. 2001; Field portable XRF analysis of environmental samples. *Journal*
642 *of Hazardous Materials.* 83, 93–122. [https://doi.org/10.1016/S0304-3894\(00\)00330-7](https://doi.org/10.1016/S0304-3894(00)00330-7).

643 Kaya, M., 2019. *Electronic Waste and Printed Circuit Board Recycling Technologies.* Springer
644 Edition: 1st. Issn: 2367-1181. <https://doi.org/10.1007/978-3-030-26593-9>.

645 Korf, N., Løvik, A.N., Figi, R., Schreiner, C., Kuntz, C., Martin Mähltitz, P., Rösslein, M., Wäger,
646 P., Rotter V.S., 2019. Multi-element chemical analysis of printed circuit boards – challenges
647 and pitfalls. *Waste Management.* 92, 124-136.
648 <https://doi.org/10.1016/j.wasman.2019.04.061>.

649 Laperche, V., Beaulieu, M., Auger, P., 2008. Caractérisation sur site et in situ de sites et sols
650 potentiellement pollués par spectrométrie de fluorescence X., *Environnement et Technique*,
651 Vol. 275, p. 37-43.

652 López-Núñez, R.; Ajmal-Poley, F.; Burgos-Doménech, P., 2020. Prediction of As, Cd, Cr, Hg, Ni,
653 and Se Concentrations in Organic Amendments Using Portable X-ray Fluorescence and
654 Multivariate Modeling. *Appl. Sci.* vol 10 (17). <https://doi.org/10.3390/app10175726>

655 Markowicz, A. 2008. Quantification and Correction Procedures. In P.J. Potts, W. West (Eds.)
656 *Portable X-Ray Fluorescence Spectrometry – Capabilities for In Situ Analysis*, RSC Publishing,
657 Cambridge. Chap. 2, 13-38.

658 Martin, J.E., Smith, L.L.A., Adjei-Bekoe, G., Thomas, R., 2010. Comparison of Different Sample
659 Preparation Procedures for the Determination of RoHS/WEEE-Regulated Elements in Printed
660 Circuit Boards and Electrical Components by EDXRF. *Spectroscopy* 25 (4), 40–45.
661 <https://doi.org/10.1016/j.wasman.2010.10.002>.

662 McWhirt, A., Weindorf, D.C., Zhu, Y., 2012. Rapid analysis of elemental concentrations in
663 compost via portable X-ray fluorescence spectrometry. *Compost Sci. Util.* 20, 185–193.
664 <https://doi.org/10.1080/1065657X.2012.10737045>.

665 Ogunniyi, I.O., Vermaak, M.K.G., Groot, D.R., 2009. Chemical composition and liberation
666 characterization of printed circuit board comminution fines for beneficiation investigations.
667 *Waste Manage.* 29 (7), 2140–2146. <https://doi.org/10.1016/j.wasman.2009.03.004>.

668 Otsuki, A., De la Mensbruge, L., King, A., Serranti, S., Fiore, L., Bonifazi, G., 2020.
669 Nondestructive characterization of mechanically processes waste printed circuit boards –

670 particle liberation analysis. *Waste Manage.* 102, 510–519.
671 <https://doi.org/10.1016/j.wasman.2019.11.006>.

672 Otsuki, A., Pereira Gonçalves, P., Leroy, E., 2019. Selective Milling and Elemental Assay of
673 Printed Circuit Board Particles for Their Recycling Purpose. *Metals.* 9, 899.
674 <https://doi:10.3390/met9080899>.

675 Potts, P.J. 2008. Introduction, Analytical Instrumentation and Application Overview. In P.J.
676 Potts, W. West (Eds.) *Portable X-Ray Fluorescence Spectrometry: Capabilities for in Situ*
677 *Analysis*. The Royal Society of Chemistry, Cambridge. UK: RSC Publishing. Chap. 1, 1-12.

678 Qiu, R., Lin, M.i., Qin, B., Xu, Z., Ruan, J., 2021. Environmental-friendly recovery of non-
679 metallic resources from waste printed circuit boards: A review. *J. Clean. Prod.* 279, 123738.
680 <https://doi.org/10.1016/j.jclepro.2020.123738>.

681 Recknagel, S., 2019. Certification report, Certified Reference Material, BAM-M505a,
682 Electronic Scrap. [https://rrr.bam.de/RRR/Content/EN/Standard-Articles/Reference-](https://rrr.bam.de/RRR/Content/EN/Standard-Articles/Reference-Materials/RM-News/rm-news-bam-m505a.html)
683 [Materials/RM-News/rm-news-bam-m505a.html](https://rrr.bam.de/RRR/Content/EN/Standard-Articles/Reference-Materials/RM-News/rm-news-bam-m505a.html). (accessed on 25 January 2022)

684 Rocchetti, L., Amato, A., Beolchini, F., 2018. Printed circuit board recycling: a patent review.
685 *J. Clean. Prod.* 178, 814–832. <https://doi.org/10.1016/j.jclepro.2018.01.076>.

686 Schneider, E.L., Hamerski, F., Veit, H.M., Krummenauer, A., Cenci, M.P., Chaves, R.D.A.,
687 Hartmann, W.L., Dias, M.D.M., Robinson, L.C., Vargas, A.S.D., 2019. Evaluation of mass loss in
688 different stages of printed circuit boards recycling employed in temperature controllers.
689 *Mater. Res.* 22,. <https://doi.org/10.1590/1980-5373-mr-2018-0833e20180833>.

690 Sharkey, M., Abdallah, M.A., Drage, D.S., Harrad, S., Berresheim, H., 2018. Portable X-ray
691 fluorescence for the detection of POP-BFRs in waste plastics. *Sci Total Environ.* 639, 49-57.
692 <https://doi.org/10.1016/j.scitotenv.2018.05.132>.

693 Thermo, Scientific,. 2010. Niton XL3t GOLDD+ Series Environmental and Mining Analyzers.
694 https://www.sirioanalytix.com/sites/default/files/XL3t%20_GOLDD.pdf. (accessed on 25
695 January 2022).

696 Thomas C. 2016. Recyclage des cartes électroniques : un aperçu de l'état de l'art
697 *Responsabilité & environnement.* n°82, 57-61.)

698 Touze, S., Guignot, S., Hubau, A., Devau, N., Chapron, S., 2020. Sampling waste printed
699 circuit boards: Achieving the right combination between particle size and sample mass to
700 measure metal content. *Waste Manag.* 118, 380-390.
701 <https://doi.org/10.1016/j.wasman.2020.08.054>.

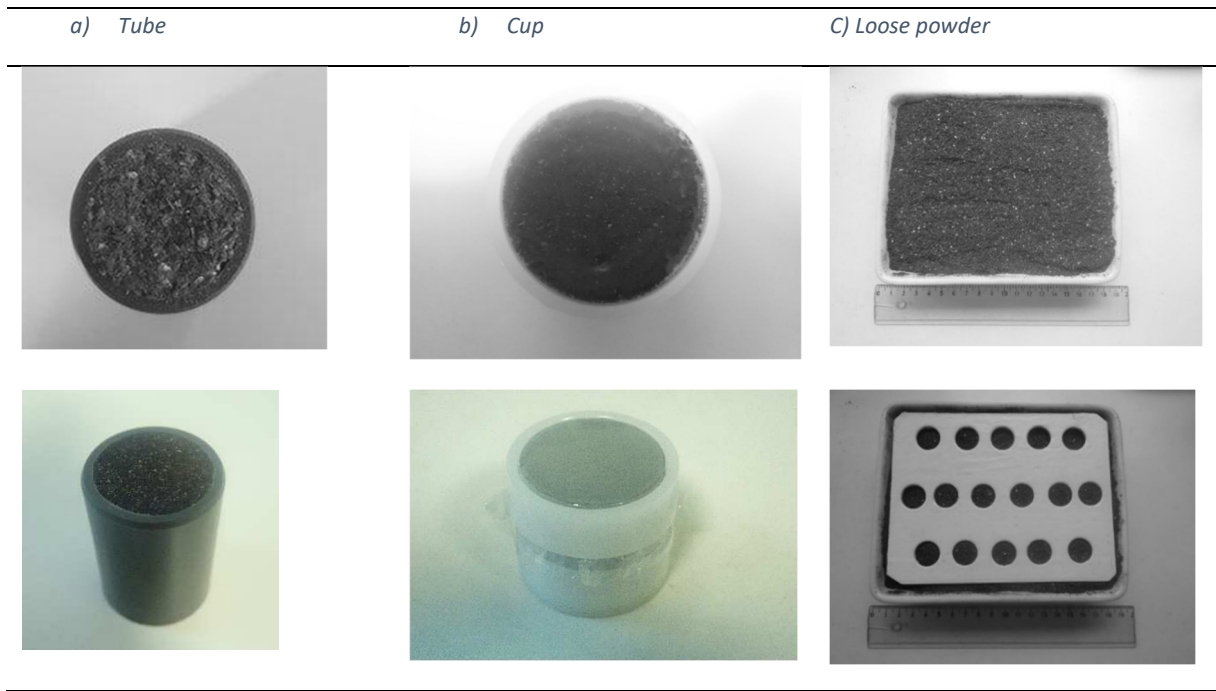
702 UMICORE, 2012. Hoboken site visit.
703 <https://www.umicore.com/storage/migrate/2012SeptHobokenSiteVisitEN.pdf>. (accessed on
704 25 January 2022).

705 UNEP., 2013. Metal Recycling: Opportunities, Limits, Infrastructure. A Report of the Working
706 Group on the Global Metal Flows to the International Resource Panel. UNEP report
707 <https://www.resourcepanel.org/reports/metal-recycling>. (accessed on 25 January 2022).

708 Wienold, J., Recknagel, S., Scharf, H., Hoppe, M., Michaelis, M., 2011. Elemental analysis of
709 printed circuit boards considering the ROHS regulations. *Waste Manag.* 31, 530–535.
710 <https://doi.org/10.1016/j.wasman.2010.10.002>.

711 Zhou, S., Yuan, Z., Cheng, Q., Weindorf, D.C., Zhang, Z., Yang, J., Zhang, X., Chen, G., Xie, S.,
712 2020. Quantitative Analysis of Iron and Silicon Concentrations in Iron Ore Concentrate Using
713 Portable X-ray Fluorescence (XRF). *Appl Spectrosc* Jan. 74(1), 55-62.
714 <https://doi.org/10.1177/0003702819871627>.

715



716 Figure 1: sample preparation procedures

717

Element	pXRF – LOD Mining mode (mg/kg)	Min and max means values ICP – analysis (mg/kg)	Interference	Applicability for studied sample
Ag	AS	155-162	Sn line overlap	No
Al	2500	59400-70000	Br line overlap	No
As	5	15.0-17.3	Pb line overlap	No
Au	20	52	Br, W, Pt, Hg lines overlap	No
Cd	10	1640-1760	Ca and Sb lines overlap	No
Co	100	333-368	Fe line overlap	No
Cr	35	759-1150	Fe line overlap	Yes
Cu	15	159000-202000		Yes
Fe	35	148000-161000		Yes
Mg	6500	1310	LOD > content	No
Mo	3	44-146		Yes
Nd	3	10.6-14.1	LOD close to content	No
Ni	30	3840-4560		Yes
Pb	10	12500-13100		Yes
Pd	5	25		Yes
Sb	15	1180-2000		Yes
Se	3	0.8-1.2	LOD > content	No
Sn	20	16700-27200		Yes
V	35	14.3-26.0	LOD > content	No
W	60	15-86	LOD > content	No
Zn	15	14500-19300		Yes

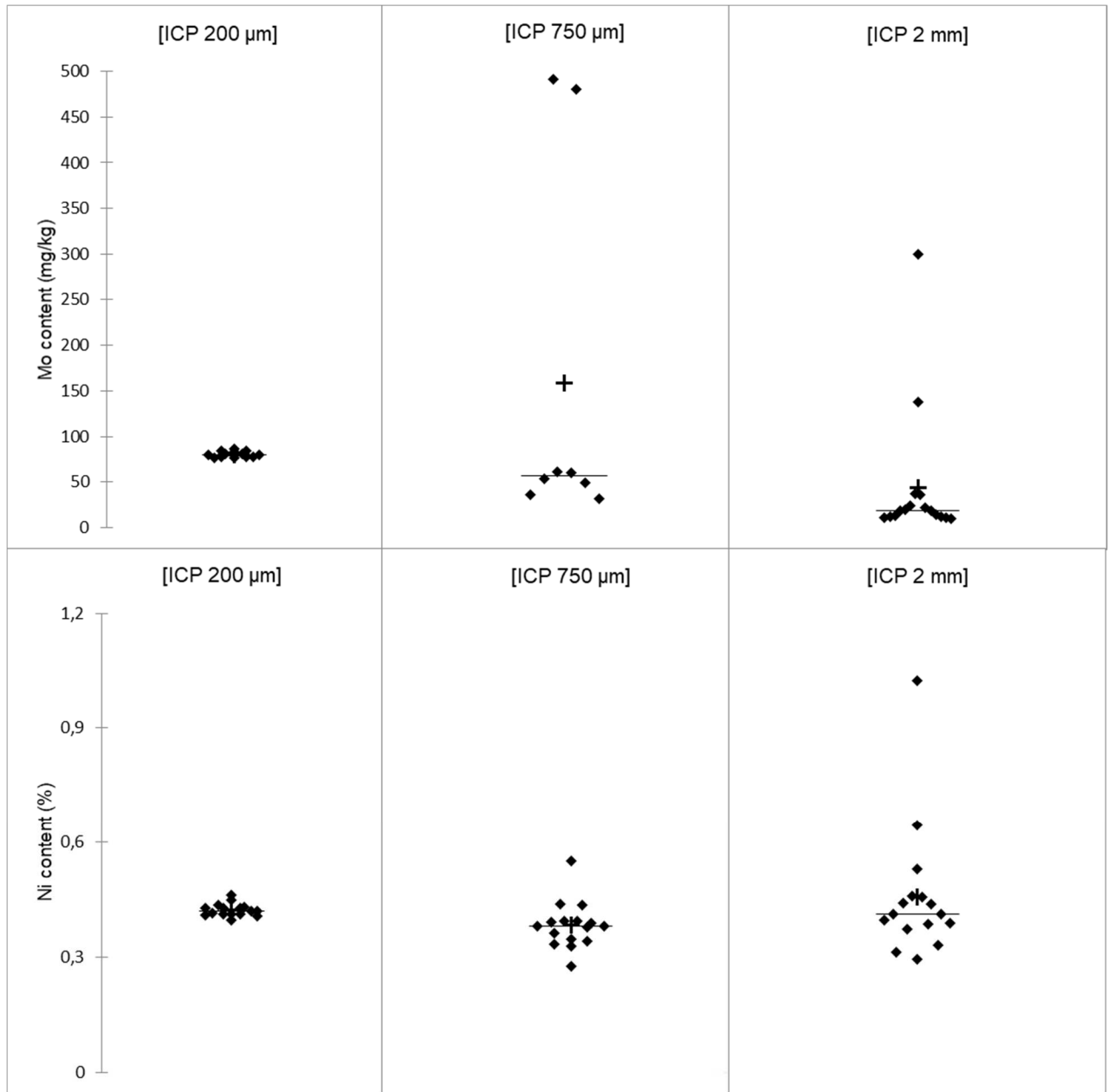
718 *Table 1 : Limit of detection in mining mode and concentrations determined by ICP analysis.*

719

Element	Unit	Number of repetitions		200 μm		750 μm		2 mm	
		200 μm /750 μm /2mm	Mean	RSD(%)	Mean	RSD(%)	Mean	RSD(%)	
Cu	%	16/16/16	20.2	3	15.9	9	17.3	7	
Fe	%	16/16/16	16.1	2	14.8	4	15.9	5	
Sn	%	16/16/16	2.46	2	1.67	16	2.72	16	
Zn	%	16/16/16	1.85	2	1.76	16	1.76	15	
Pb	%	16/16/16	1.25	2	1.29	12	1.31	16	
Ni	mg/kg	16/16/16	4226	4	3824	16	4560	38	
Sb	mg/kg	16/8/16	1742	1	2048	2	1185	11	
Cr	mg/kg	16/8/16	1151	4	842	12	759	34	
Mo	mg/kg	16/8/16	80	4	158	122	44	171	
Pd	mg/kg	0/16/0			24.9	37			

720 *Table 2: Mean values from [ICP 200 μm], [ICP 750 μm] and [ICP 2 mm](aqua regia digestion – mass digested =5g).*

721



723

724

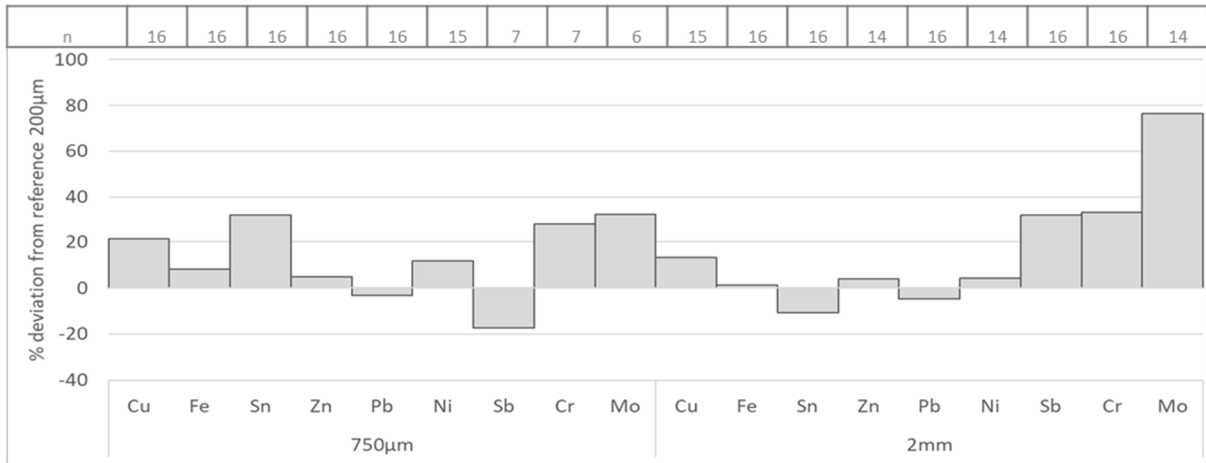
725

Figure 2 : Scattergrams for Mo and Ni ([ICP 200 μm], [ICP 750 μm] and [ICP 2 mm]) (♦ measurements, + mean value and — median value)

726

727

728



729

730

Figure 3: [ICP 750 μm] and [ICP 2mm] deviation from the reference value ([ICP 200 μm]);. n= number of repetitions after exclusion of erratic points

731

732

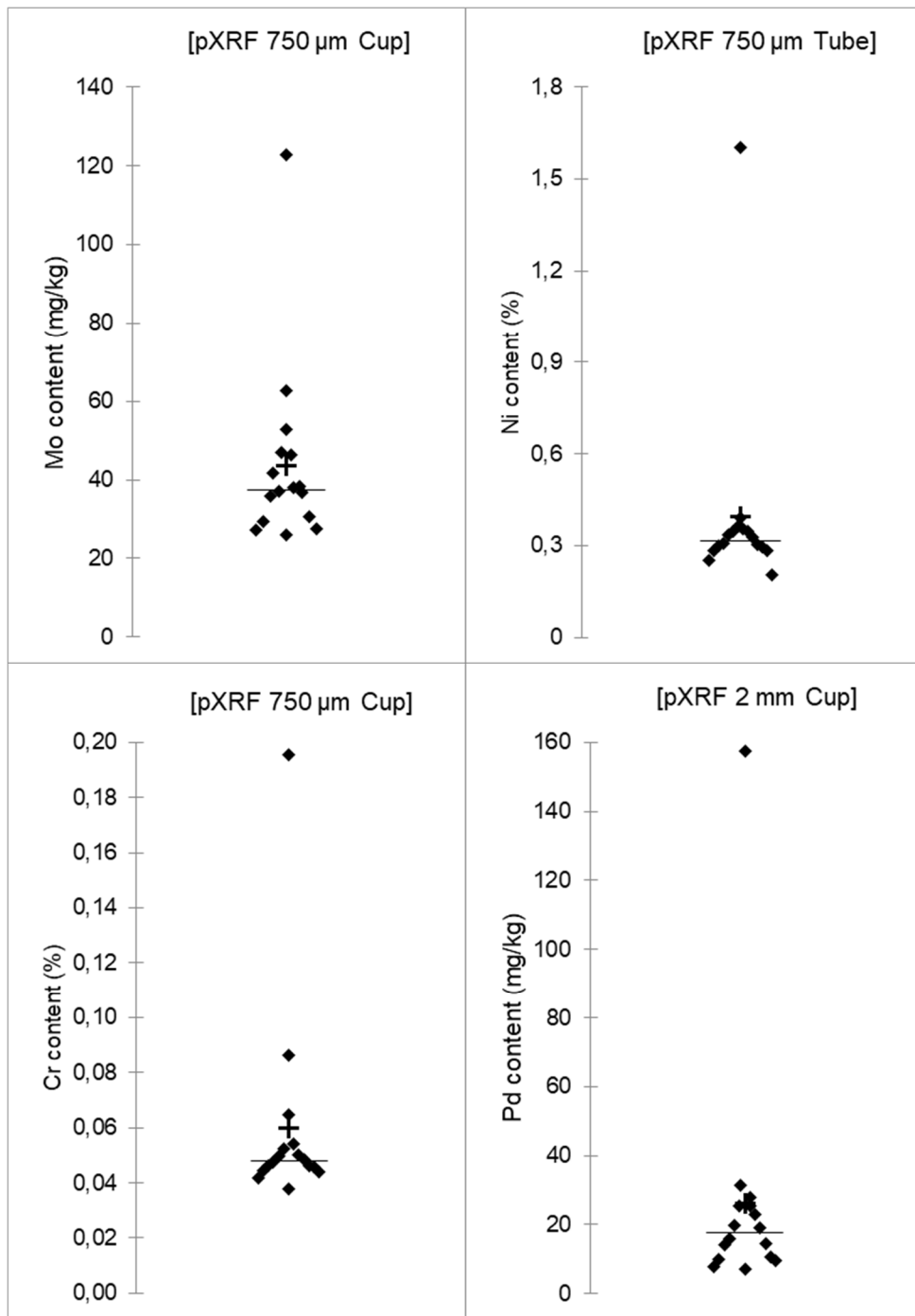
733

Particle-size		200 μm						750 μm						2 mm					
Condition		Tube		Cup		Loose powder		Tube		Cup		Loose powder		Cup		Loose powder			
Element	Unit	Mean	RSD(%)	Mean	RSD(%)	Mean	RSD(%)	Mean	RSD(%)	Mean	RSD(%)	Mean	RSD(%)	Mean	RSD(%)	Mean	RSD(%)		
Cu	%	16,8	2	16,3	4	16,0	5	12,0	15	11,80	24	9,9	41	9,9	27	6,5	48		
Fe	%	11,9	2	11,5	2	11,6	4	8,4	25	9,65	20	7,0	34	7,3	41	5,0	54		
Sn	%	2,1	3	2,1	2	2,0	7	1,3	21	1,18	24	1,0	34	0,9	39	0,5	51		
Zn	%	2,1	3	2,0	3	2,0	7	1,1	24	1,22	29	0,9	36	0,9	65	0,7	109		
Pb	%	1,2	3	1,2	2	1,20	5	0,8	24	0,81	21	0,7	35	0,6	36	0,3	55		
Ni	mg/kg	3719	4	3727	8	3724	5	3937	83	3610	46	3159	34	3461	58	2551	96		
Sb	mg/kg	2622	3	2587	4	2572	9	2467	15	2380	9	2328	33	2285	29	2566	50		
Cr	mg/kg	910	7	885	6	855	14	507	25	597	64	419	31	282	41	140	38		
Mo	mg/kg	89	16	81	17	79	14	43	23	44	53	38	66	16	47	17	72		
Pd	mg/kg	21	19	20	16	23	22	27	81	17	44	19	46	29	130	13	23		

734 *Table 3 : Mean values for the [pXRF 200 μm Tube/Cup/Powder], [pXRF 750 μm Tube/Cup/Powder] and [pXRF 2 mm Cup/Powder]*

735

736

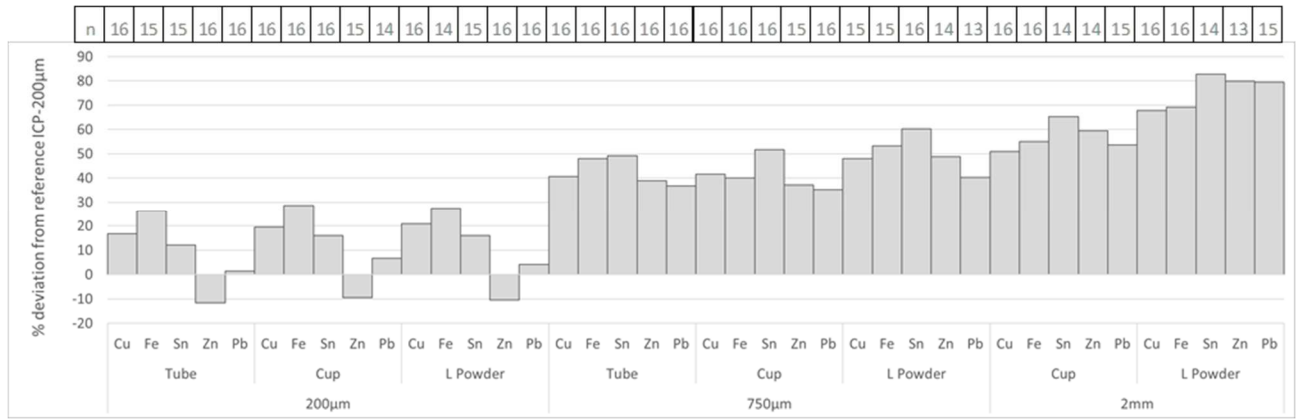


738

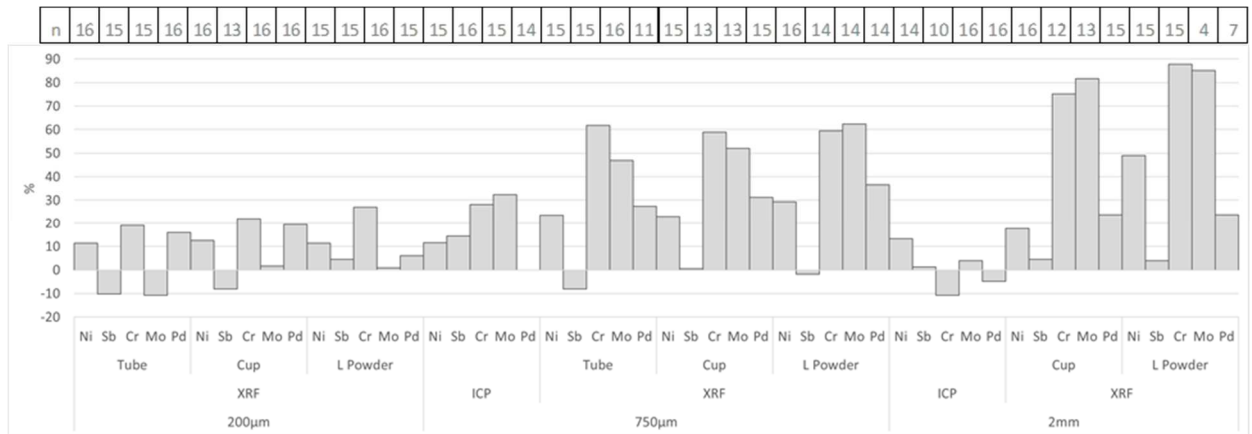
739 Figure 4 : Scattergrams for Mo [pXRF 750 μ m Cup], Ni [pXRF 750 μ m Tube], Cr [pXRF 750 μ m Cup] and Pd [pXRF 2 mm
740 Cup](♦ measurements, + mean value and — median value)

741

742



743



744 Figure 5 : pXRF deviation from the reference value [ICP 200 µm]; n= number of repetitions after exclusion of erratic points

745